2022

# Adopting Scenario-Based approach to solve optimal reactive power Dispatch problem with integration of wind and solar energy using improved Marine predator algorithm

Noor Habib Khan

Raheela Jamal

Mohamed Ebeed

*See next page for additional authors*


Funder: European Union; Enterprise Ireland; National Research and Development Agency of Chile (ANID)

## Authors

Noor Habib Khan, Raheela Jamal, Mohamed Ebeed, Salah Kamel, Hamed Zeinoddini-Meymand, and Hossam Zawbaa

Ain Shams Engineering Journal 13 (2022) 101726

Contents lists available at ScienceDirect

Ain Shams Engineering Journal

journal homepage: www.sciencedirect.com

# Adopting Scenario-Based approach to solve optimal reactive power Dispatch problem with integration of wind and solar energy using improved Marine predator algorithm

Noor Habib Khan [a], Raheela Jamal [b], Mohamed Ebeed [c], Salah Kamel [d], Hamed Zeinoddini-Meymand [e], Hossam M. Zawbaa [f,g,*]

[a] School of New Energy, North China Electric Power University, Beijing 102206, China
[b] School of Control & Computer Engineering, North China Electric Power University, Beijing 102206, China
[c] Department of Electrical Engineering, Faculty of Engineering, Sohag University, Sohag 82524, Egypt
[d] Department of Electrical Engineering, Faculty of Engineering, Aswan University, Aswan 81542, Egypt
[e] Department of Electrical and Computer Engineering, Graduate University of Advanced Technology, Kerman, Iran
[f] Faculty of Computers and Artificial Intelligence, Beni-Suef University, Beni-Suef, Egypt
[g] Technological University Dublin, Dublin, Ireland

ARTICLE INFO

*Article history:*
Received 1 November 2021
Revised 26 December 2021
Accepted 28 January 2022

*Keywords:*
Marine Predator Algorithm
Optimal Reactive Power Dispatch
Photovoltaic Power
Renewable Energy Resources
Scenario-based Approach

ABSTRACT

The penetration of renewable energy resources into electric power networks has been increased considerably to reduce the dependence of conventional energy resources, reducing the generation cost and greenhouse emissions. The wind and photovoltaic (PV) based systems are the most applied technologies in electrical systems compared to other technologies of renewable energy resources. However, there are some complications and challenges to incorporating these resources due to their stochastic nature, intermittency, and variability of output powers. Therefore, solving the optimal reactive power dispatch (ORPD) problem with considering the uncertainties of renewable energy resources is a challenging task. Application of the Marine Predators Algorithm (MPA) for solving complex multimodal and non-linear problems such as ORPD under system uncertainties may cause entrapment into local optima and suffer from stagnation. The aim of this paper is to solve the ORPD problem under deterministic and probabilistic states of the system using an improved marine predator algorithm (IMPA). The IMPA is based on enhancing the exploitation phase of the conventional MPA. The proposed enhancement is based on updating the locations of the populations in spiral orientation around the sorted populations in the first iteration process, while in the final stage, the locations of the populations are updated their locations in adaptive steps closed to the best population only. The scenario-based approach is utilized for uncertainties representation where a set of scenarios are generated with the combination of uncertainties the load demands and power of the renewable resources. The proposed algorithm is validated and tested on the IEEE 30-bus system as well as the captured results are compared with those outcomes from the state-of-the-art algorithms. A computational study shows the superiority of the proposed algorithm over the other reported algorithms.



## 1. Introduction

The electric power networks are complicated networks and consist of generation, distribution and transmission arrangements that aim to operate in a secure and economic environment with minimization of transmission losses, voltage profile and operational cost, as well as enhancing the voltage stability. It is possible to achieve these optimization objectives by selecting the suitable coordination of operational variables such as transformer tap settings and generator output voltages as well as shunt reactive

* Corresponding author at: Technological University Dublin, Park House, 191 N Circular Rd, Cabra East, Grangegorman, Dublin D07 EWV4, Ireland.
*E-mail addresses:* noorhabibkhan@ncepu.edu.cn (N. Habib Khan), raheelajamal@ncepu.edu.cn (R. Jamal), mebeed@eng.sohag.edu.eg (M. Ebeed), skamel@aswu.edu.eg (S. Kamel), h.zeinoddini@kgut.ac.ir (H. Zeinoddini-Meymand), hossam.zawbaa@gmail.com (H.M. Zawbaa).

Peer review under responsibility of Ain Shams University.

Production and hosting by Elsevier

https://doi.org/10.1016/j.asej.2022.101726

VAR compensators, respectively [1]. ORPD is a non-convex and non-linear model that contains continuous and discrete decision variables. The new trend of incorporating renewable energy resources (RERs) is extensively used in the power system to provide a sophisticated solution in terms of technical, economic and environmental perspectives [2]. The generation from these resources can reduce the dependency on fossil fuel, minimize generation cost, improve the system operation, reduce greenhouse gases and harmful emissions [66,67].

### 1.1. Literature review

The ORPD problem can be solved via using different classical techniques such as; interior-point [3], linear [4] and non-linear programming [5], quadratic programming [6] and Newton-Rapson [7], respectively. These techniques face problems while using for large-scale systems such as; trapping in local minima and complex computation. To solve these optimization issues, the researchers developed new *meta*-heuristic techniques to resolve these non-linear optimization problems of ORPD. For solving the conventional thermal problem, the different *meta*-heuristic optimization techniques are considered to solve the ORPD problem, such as; moth-flame optimization [8], genetic algorithm [9], sine cosine algorithm [10], grey wolf optimizer [11], barnacles mating optimizer [12], Bat algorithm [13], artificial bee colony algorithm [14], Jaya algorithm [15], particle swarm optimization [16], θ-social mimic optimization [17], bamboo plant intellect deeds optimization [18], levy flight based white wolf algorithm [19], whale optimization algorithm [20], ant lion optimizer [21], wind-driven optimization Algorithm [22], modified-differential evolution algorithm [23], comprehensive learning particle swarm optimization [24], biogeography-based optimization [25] and hybrid Fuzzy-Jaya optimizer [26].

The most type of RERs used for the integration of ORPD solutions are solar and wind power. However, these resources have some technical deficiencies due to their stochastic behavior and continuously varying that can cause uncertainty in the electrical power networks. However, it has mostly seemed in terms of fluctuations in load demand [27]. So, it's a spiritual task for the decision-maker to plan these resources in the electrical power networks efficiently. Hence, there are several techniques modelled for these problems, such as hybrid possibilistic–probabilistic methods [28], interval analysis [29], probabilistic methods [30] and robust optimization [31], respectively. The relevant latest studies have been included in the literature related to the integration of RERs in ORPD to understand the significance of these resources in the power systems. Fractional calculus-based PSOGSA algorithm discussed in [32] to solve ORPD with taking into account the uncertainty of RERs generation. ORPD solution using Moth Swarm Algorithm is discussed in [33] to minimize the power losses using uncertainty in RERs. RAO-3 algorithm in [34] considering the uncertain PV and Wind resources with a time-varying load. SHADE algorithm [35], used to solve ORPD problem with the inclusion of uncertainty in RERs and load demand. ECOA algorithm is presented in [36], considering the wind units and solving the ORPD problem. Moreover, LAPO and improved LAPO techniques are used to solve the ORPD problem [37,38] with the integration of solar and wind under uncertainty of the load demand to minimize the power losses using IEEE 30 standard.

The marine predator algorithm is an efficient and recently developed algorithm introduced by A. Faramarzi et al. in 2020 [39]. It is used in some engineering applications such as; parameter estimation of PV models [40], image segmentation [41], the parameter of identification of triple-diode PV model [42], ranking based diversity reduction strategy [43], forecasting of COVID-19 [44] and parameter estimation of fuel cell [45], respectively. For some cases, the traditional MPA may face the stagnation problem and trap into the local minima. The research presented the novel modified MPA algorithm based on using levy flight distribution (LFD) concept and spiral movement of predators to global solution helps to improve the exploration and exploration properties of the algorithm.

### 1.2. Research contribution

The main research contributions can be depicted as follows:

- Solving the ORPD problem considering PV and Wind energy with time-varying load.
- The improved marine predator algorithm (IMPA) is introduced based on predator mutation strategy and spiral movement to enhance exploration and exploitation mechanisms.
- The IMPA was applied to resolve the ORPD problem with and without considering RERs applied on IEEE 30 standard.
- To authenticate the efficiency of the proposed IMPA, the results are compared to the different *meta*-heuristic approaches.

The paper organization is arranged as follows: the mathematical formulation of ORPD problem is present in Section 2, formulation related uncertainties in RERs are presented in Section 3, Methodology of the IMPA is introduced in Section 4, results and discussions are offered in Section 5, while Section 6 is part of the conclusion

## 2. Problem formulation of ORPD

The ORPD problem solution aims to determine the set of control parameters for system performance enhancement to satisfy the operational constraints. Usually, the mathematical expression of ORPD can be expressed according to the following equations:

$$MinF(x,u) \tag{1}$$

Subjected to

$$g_{eq}(x,u) = 0k = 1,2,\cdots,m \tag{2}$$

$$h_{ieq}(x,u) \le 0n = 1,2,\cdots,p \tag{3}$$

where $g_{eq}$ and $h_{ieq}$ are representing the terms related to equality and inequality constraints. $u$ is vector referring to control parameters, including the generator voltages ($V_G$), the reactive power of capacitors ($Q_C$), the transformer taps ($T_p$), whereas $x$ refers to the dependent variables and slack bus power, the transmission lines power flow ($S_T$), voltages of the load buses ($V_L$) and the reactive generators power ($Q_G$). The vectors $u$ and $x$ are represented as follows:

$$u = [Q_C, T_p, V_G] \tag{4}$$

$$x = [S_T, Q_G, V_L, P_1] \tag{5}$$

### 2.1. Objective function

#### 2.1.1. Power losses

The first objective is to minimize the transmission line losses and its formulation is given as follows:

$$F_1 = P_{Losses} = \sum_{i=1}^{N_L} G_{ij}(V_i^2 + V_j^2 - 2V_iV_jcos\delta_{ij}) \tag{6}$$

where, $G_{ij}$ is the conductance of the transmission line, $V_i$ and $V_j$ are the voltage magnitudes whereas, $N_L$ is the number of transmission lines.

*2.1.2. Voltage Deviation*

The second objective is to minimize the voltage deviations and improve the voltage profile. It is related to the quality of the voltages in the electrical networks and computed as adding of voltage deviations of the load buses compared to the reference voltage which is equal to 1. The related formulation is usually expressed as follows:

$$F_2 = VD(p.u) = \sum_{i=1}^{N_q} |(V_i - 1)| \tag{7}$$

Where, $N_q$ represents the number of load buses, $V_i$ is the bus voltage of the i-th load bus.

*2.1.3. Voltage stability enhancement*

The third objective is to improve voltage stability, which is considered the utmost perilous phenomenon due to voltages instability in the electrical power networks. The voltage instability can cause voltage collapse steadily or suddenly in the electrical power network and is required to improve. The voltage stability is denoted as L-index of each bus and can be enhanced by the L-index values at one bus formulated as:

$$F_3 = minL_i = \left| 1 - \frac{\sum_{j=1}^{ng} y_{ij} v_j}{v_i} \right| i = 1, 2, \cdots, N_{bus} \tag{8}$$

$$F_3 = \min L_{max} i = 1, 2, \cdots, N_{bus} \tag{9}$$

where, $L_i$ is the value of stability index of i-th bus, whereas $y_{ij}$ is the mutual admittance between i and j.

*2.2. Constraints*

*2.2.1. Equality constraints*

$$P_{Gi} - P_{Li} = |V_i| \sum_{j=1}^{NB} |V_j| \left(G_{ij} cos\delta_{ij} + B_{ij} sin\delta_{ij}\right) \tag{10}$$

$$Q_{Gi} - Q_{Li} = |V_i| \sum_{j=1}^{NB} |V_j| \left(G_{ij} sin\delta_{ij} - B_{ij} cos\delta_{ij}\right) \tag{11}$$

*2.2.2. Inequality constraints*

$$P_{G,k}^{min} \le P_{G,k} \le P_{G,k}^{max} k = 1, 2, \cdots, N_G \tag{12}$$

$$Q_{G,k}^{min} \le Q_{G,k} \le Q_{G,k}^{max} k = 1, 2, \cdots, N_G \tag{13}$$

$$V_{G,k}^{min} \le V_{G,k} \le V_{G,k}^{max} k = 1, 2, \cdots, N_G \tag{14}$$

$$T_{p,n}^{min} \le T_{p,n} \le T_{p,n}^{max} n = 1, 2, \cdots, N_p \tag{15}$$

$$Q_{C,n}^{min} \le Q_{c,n} \le Q_{c,n}^{max} n = 1, 2, \cdots, N_c \tag{16}$$

$$S_{T,n} \le S_{T,n}^{min} n = 1, 2, \cdots, N_T \tag{17}$$

$$V_{L,n}^{min} \le V_{L,n} \le V_{L,n}^{max} n = 1, 2, \cdots, N_q \tag{18}$$

Where *min* and *max* are superscripts denote the upper and the lower limits. $N_G$, $N_p$, $N_c$, $N_L$ and $N_q$ are the number of generators, transformers, capacitors, transmission lines and load buses, respectively. The obtained solution must be at the appropriate solution. To ensure this, the weighted square variables expression is used as follows:

$$F = F_i + \chi_1 \left(P_{G1} - P_{G1}^{lim}\right)^2 + \chi_2 \sum_{i=1}^{N_G} \left(Q_{Gi} - Q_{Gi}^{lim}\right)^2 + \chi_3 \times \sum_{i=1}^{N_q} \left(V_{Li} - V_{Li}^{lim}\right)^2 + \chi_4 \sum_{i=1}^{N_L} \left(S_{Li} - S_{Li}^{lim}\right)^2 \tag{19}$$

where $F$ represents the penalty factor while $\chi_1, \chi_2, \chi_3$ and $\chi_4$ are the coefficient of the penalty factors. The values of the penalty coefficients $\chi 1$, $\chi 2$, $\chi 3$ and $\chi 4$ are selected to be 100, 100, 1000 and 100, respectively.

## 3. Uncertainty modeling

The Continuous Probability Function (PDF) is for modelling the uncertainty of the system, which includes uncertainty in the load demand, the output of solar PV and the wind power generation system. The PDF is further divided into subsections in order to get the different scenarios of loading, wind speed and solar PV [46].

*3.1. Load demand modeling*

To modelled the uncertainty of the load demand by using the PDF [34], it is defined as follows:

$$f_d(P_d) = \frac{1}{\sigma_d \sqrt{2\pi}} exp\left[ - \frac{(P_d - \mu_d)2}{2\sigma_d^2} \right] \tag{20}$$

Where, $\mu_d$ and $\sigma_d$ are indicated the mean and the standard deviations parameters, whereas, $P_d$ represents probability density of normal distribution load, respectively. In addition, the load demand probability with its related expected load scenario generation can be formulated as follows [33].

$$\tau_i^d = \int_{P_{d,i}^{min}}^{P_{d,i}^{max}} \frac{1}{\sigma_d \sqrt{2\pi}} exp\left[ - \frac{(P_d - \mu_d)2}{2\sigma_d^2} \right] dP_d \tag{21}$$

$$P_{d,i} = \frac{1}{\tau_{d,i}} \int_{P_{d,i}^{min}}^{P_{d,i}^{max}} \frac{P_d}{\sigma_d \sqrt{2\pi}} exp\left[ - \frac{(P_d - \mu_d)2}{2\sigma_d^2} \right] dP_d \tag{22}$$

where $P_{d,i}^{max}$ and $P_{d,i}^{min}$ are the upper and the lower limits of the selected interval of *i-th*. It is mentioned that the value of the $\sigma_d$ considered in the paper is $0.02\mu_d$. The detail of load scenarios and their probabilities are given in Table 1.

*3.2. Solar irradiation modeling*

The Beta PDF is used to model the uncertainty in solar irradiance, which is denoted as $G_S$ [34]. However, Beta PDF formulation can be given as follows:

**Table 1**
Generation of Wind, Solar and the Load Scenarios with their Probabilities.

| **Scenarios of Load** | **Loading %** | $\tau_{d,i}$ |
|---|---|---|
| 1 | 58.5892 | 0.3085 |
| 2 | 72.0663 | 0.5328 |
| 3 | 85.2514 | 0.1587 |
| **Scenarios of Wind Speed** | **Wind Speed %** | $\tau_{wind,k}$ |
| 1 | 5.3953 | 0.6321 |
| 2 | 11.1082 | 0.2789 |
| 3 | 16.4918 | 0.0889 |
| **Scenarios of Solar Irradiance** | **Solar Irradiance %** | $\tau_{solar,m}$ |
| 1 | 691.4611 | 0.1255 |
| 2 | 857.2083 | 0.1671 |
| 3 | 970.6447 | 0.7075 |

$$f_G(G_S) = \begin{cases} \frac{\Gamma(\alpha+\beta)}{\Gamma(\alpha)+\Gamma(\beta)} \times G_s^{\alpha-1} \\ \times(1-G_S)^{\beta-1} \quad If 0 \le G_S \le 1, 0 \le \alpha, \beta \\ 0 otherwise \end{cases} \tag{23}$$

here, $\alpha$ and $\beta$ represents the beta probability parameters which can be computed in terms of standard deviations ($\sigma_s$) and mean ($\mu_s$) of the random variables given as follows:

$$\beta = (1-\mu_s) \times \left(\frac{\mu_s \times (1+\mu_s)}{{\sigma_s}^2}\right) - 1 \tag{24}$$

$$\sigma_s = (1-\mu_s) \times \left(\frac{\mu_s \times \beta}{(1-\mu_s)}\right) - 1 \tag{25}$$

The generated output of the PV system is computed as the solar irradiance function and can be formulated as follows [34,46]:

$$P_s(G_S) = \begin{cases} P_r\left(\frac{G_s^2}{G_{std} \times X_c}\right) for 0 < G_S \le X_c \\ P_r\left(\frac{G_S}{G_{std}}\right) for G_S \ge X_c \end{cases} \tag{26}$$

here,$P_s$ is the output of solar-PV, $P_r$ is the rated power, $G_{std}$ is the standard solar irradiance with a value considered 1000 W/m$^2$. Moreover, the certain irradiance point is denoted by $X_c$ with the value considered 120 W/m$^2$ [50]. The 50 MW rated power of the solar-PV is considered in this research which is connected to generator bus 8 of IEEE 30-bus standard. The solar irradiance probability of each scenario can be computed as follows [32].

$$P_s(G_S)\tau_m^{Solar} = \int_{G_m^{min}}^{G_m^{max}} f_{G_s}(G_S) dG_S \tag{27}$$

where $\tau_m^{Solar}$ presents the probability of solar being in scenario $m$. $G_m^{min}$ and $G_m^{max}$ are the ending and the starting points of solar irradiance interval at $m^{th}$ scenario. In this paper, three scenarios are generated related to solar irradiance by using (27). The corresponding probability and solar irradiance scenarios are given in Table 1.

### 3.3. Wind speed modeling

The Weibull Probability Distribution Function (PDF) is considered here to modelled the uncertainty of the wind speed (m/sec); the expression is given as follows [32]:

$$f_u(u) = \left(\frac{\beta_{shape}}{\alpha_{scale}}\right)\left(\frac{u}{\alpha_{scale}}\right)^{(\beta_{shape}-1)} exp\left[-\left(\frac{u}{\alpha_{scale}}\right)^{\beta_{shape}}\right] \qquad 0 \leqslant u < \infty \tag{28}$$

Where $\beta_{shape}$ and $\alpha_{scale}$ are represented as the shape and scale parameters of Weibull distribution. To find the output power of a wind turbine, the related expression can be as followed [49]:

$$P_w(u_\omega) = \begin{cases} 0 & for \quad (u_\omega < u_{\omega i} \& u_\omega > u_{\omega o}) \\ P_{rated}\left(\frac{u_\omega - u_{\omega i}}{u_{\omega r} - u_{\omega i}}\right) & for \quad (u_{\omega i} \le u_\omega \le u_{\omega r}) \\ P_{rated} & for \quad (u_{\omega r} < u_\omega \le u_{\omega o}) \end{cases} \tag{29}$$

here, $P_w$ is the output of the wind turbine, $u_{\omega o}$, $u_{\omega r}$ and $u_{\omega i}$ are the cut-out, rated and the cut-in speed with the values 25, 16 and 3 m/sec, respectively [33]. While, $P_{rated}$ is rated power of the wind turbine. In our study case, the total power output taken from the wind farm is 75 MW, in which 25 turbines are connected with rated 3 MW power of each turbine. The probability of the wind speed can be computed as follows [34].

$$\tau_k^{wind} = \int_{u_k^{min}}^{u_k^{max}} f_u(u) du \tag{30}$$

Here,$u_k^{max}$ and $u_k^{min}$ are the ending and the starting points of wind speed interval at k-th scenario. $\tau_k^{wind}$ denoted the probability of wind being in k-th scenario. The scenarios of wind speed with their probabilities are given in Table. 1.

### 3.4. Combined load generation modeling

The corresponding probabilities for load demand, solar irradiance and wind speed models are given in Table 1; while combining the model of three functions will be captured by multiplying their probabilities, the related expression is given as follows [46]:

$$\tau_S = \tau_i^{dm} \times \tau_k^{wind} \times \tau_m^{Solar} \tag{31}$$

## 4. Optimization algorithm

### 4.1. Marine Predators' algorithm (MPA)

The traditional MPA is an efficient technique inspired by the scavenging action of marine predators such as; sunfish, swordfish, tunas, marlines and sharks with their prey in the ocean. The scavenging technique depends on two random movements like Brownian movements and Lévy flight walk, which is presented in Fig. 1. Humphries et al. [47] indicated Lévy's motion which has an extensive outline among the marine predators', when searching for food. However, when it is in a state of scavenging, the pattern usually converts into the Brownian type. It is worst mentioning here that the Lévy flight walk is an arbitrary technique of change-over of a particle from one spot to another spot which is working on the probability distribution function [39].

In a prey-sparse environment, the movement of the predators to the food is based on Lévy flight walk, while in a pre-abundant area, the movement of the predators is based on a Brownian pattern. In addition, the other behavior is also considered due to the movement of sharks, named, Fish aggregating device (FAD), and it revealed that the sharks move in a sudden vertical jump. The steps of the MPA can be depicted as follows:

**Step 1:** initialization

In this step, a set of populations are generated randomly as follow:

$$X_i = X_i^{min} + \left(X_i^{max} - X_i^{min}\right) \times Rand \tag{32}$$

where $X_i^{min}$ is the lower limit of the $i^{th}$ population while $X_i^{max}$ denotes its upper limit, whereas *Rand* presents the random value which range is between $0 \le Rand \le 1$. Then evaluate the fitness function for each population as follows:

$$F_i = obj(X_i) \tag{33}$$

**Step 2:** Determination of the top predator

In this step, the obtained populations are organized in a matrix (the prey matrix) as follows:

$$X = \begin{bmatrix} X_{1,1} & X_{1,2} & \cdots & X_{1d} \\ X_{2,1} & X_{22} & \cdots & X_{2,1} \\ \vdots & \vdots & \ddots & \vdots \\ X_{n,1} & X_{n,2} & \cdots & X_{n,d} \end{bmatrix} \tag{34}$$

Here, $n$ refers to the number of entire populations, $d$ denoted the number of the dimensions. The organization of solutions assigns the best predator according to their objective function values. Therefore, another matrix is constructed named Elite matrix, which includes the topmost predators as follows:

$$Elite = \begin{bmatrix} E_{1,1} & E_{1,2} & \cdots & E_{1d} \\ E_{2,1} & E_{22} & \cdots & E_{2,1} \\ \vdots & \vdots & \ddots & \vdots \\ E_{n,1} & E_{n,2} & \cdots & E_{n,d} \end{bmatrix} \quad (35)$$

**Step 3:** The Brownian and Lévy Flight orientation

The placement of predators and the preys are updated in the three phases that depend on their velocity relation between prey and predator velocity. The detail of MPA phases is given below.

**Phase 1:** This phase is the exploration phase and functional at the highest velocity ratio, which means the prey's velocity is lower than the predator's velocity. The predator and the prey are updated their states through Brownian motion as follows:

$$\overline{SZ_i} = \overline{R_{Br}} \oplus (\overline{E_i} - \overline{R_{Br}} \oplus \overline{X_i}) if T \le T_{max} \quad (36)$$

$$\overline{X_i} = \overline{X_i} + P.\bar{R} \oplus \overline{SZ_i} \quad (37)$$

Where, $\bar{SZ_i}$ is the step size vector. $\bar{R_{Br}}$ vector is represented as the Brownian motion that contains random numbers, $T$ and $T_{max}$ are the present and maximum iterations number, $\oplus$ is the entry wise multiplication factor while P is the constant value equals to 0.5.

**Phase 2:** It is an intermittent phase among the exploitation and exploration phases that will be functional when the velocity of prey is equal to the velocity of the predator. The populations are separated into two sets; the first set is exploited while the latter is set for exploration. For this phase, the following expression can be written as:

The first group or exploitation group

$if \frac{1}{3}T_{max} \le T \le \frac{2}{3}T_{max}$

$$\overline{SZ_i} = \overline{R_{Levy}} \oplus (\overline{E_i} - \overline{R_{Levy}} \oplus \overline{X_i}) for i = 1, 2, 3, .., \frac{n}{2} \quad (38)$$

$$\overline{X_i} = \overline{X_i} + P.\bar{R} \oplus \overline{SZ_i} \quad (39)$$

The second group or exploration group

$$\overline{SZ_i} = \overline{R_{Br}} \oplus (\overline{E_i} - \overline{R_{Br}} \oplus \overline{X_i}) for i = \frac{n}{2}, \cdots, n \quad (40)$$

$$\overline{X_i} = \overline{X_i} + P.CF \oplus \overline{SZ_i} \quad (41)$$

Here, $\bar{R_{Levy}}$ denotes a vector that includes the random numbers produced using the Lévy distribution that imitators the drive of the prey in the levy manner. While, $CF$ is an adaptive operator which aims to control the step size of the predator's drive.

**Phase 3:** This is an entire exploitation phase that will be imposed when the velocity of prey is less than the predators' velocity at the final stages.

$$\overline{SZ_i} = \overline{R_{Levy}} \oplus (\overline{R_{Levy}} \oplus \overline{E_i} - \overline{X_i}) for i = 1, 2, 3 \cdots, \frac{n}{2} \quad (42)$$

$$\overline{X_i} = \overline{E_i} + P.\bar{R} \oplus \overline{SZ_i} \quad (43)$$

The predators in this phase are moved by the levy approach. The above equations describe the prey's velocity based on the Elite vector.

**Step 4:** The movement behavior of the predators is effect by environmental issues. The predators move in fish aggregating devices or eddy formations that represent the local optima. While to find the new environment, they take a long jump which has abundant the regions. The expression related to this step is given as follows:

$$\overline{X_i} = \begin{cases} \bar{X_i} + CF \begin{bmatrix} X_i^{min} + \\ R\left(X_i^{max} - X_i^{min}\right) \end{bmatrix} \oplus U^- \; If r \le FADS \\ \overline{X_i} + \begin{bmatrix} FADS(1-r) + \\ r \end{bmatrix} (X_{r1}{}^- - X_{r2}{}^-) If r > FADS \end{cases} \quad (44)$$

Where $\bar{U}$ is a binary vector, $r1$ and $r2$ are the random values from prey matrix, $r$ presents the random number range between [0,1], FADS is the fish aggregating devices probability and its' value is equal to 0.2, respectively.

**Step 5:** Marine memory

For the best foraging solution, the marine predators remember their location efficiently. However, in MPA, the updated population is compared with previous populations based on their objective function to capture the global solution.

### 4.2. Improved Marine Predators' algorithm (IMPA)

The IMPA is proposed to enhance the searching capabilities of the traditional MPA by enhancing the exploitation phase. The exploitation phase of the algorithm is enhanced by the spiral movement of the predators around the elite solutions as follows:

The first step of modification in traditional MPA is based on spiral orientation is expressed as follows:

$$\overline{X_i} = (\overline{E_i} - \overline{X_i}) \times e^{bt} cos(2\pi T) + \overline{E_i} \quad (45)$$

where $b$ denoted as a constant, which describe the logarithmic spiral shape. Then at the final stage of the iteration process, the predators updated their location around only the best solution using adaptive operators:

**If rand < 0.5**

$$\overline{X_i} = \overline{E_i} + Bw \times r3 \quad (46)$$

**Else**

$$\overline{X_i} = \overline{E_i} - Bw \times r3 \quad (47)$$

**End**

where $r3$ is a random value in the range [0–1]. $Bw$ is a variable parameter decreasing dynamically as follows:

$$w(t) = Bw_{max} \times e^{(C \times T)} \quad (48)$$

$$C(t) = \left( ln(\frac{Bw_{min}}{Bw_{max}}) / T_{max} \right) \quad (49)$$

where $Bw_{min}$ and $Bw_{max}$ are the minimum and the maximum limits of $Bw$.

The values of the $Bw_{min}$ and $Bw_{max}$ are selected to be 0.1 and 0.001, respectively. These values are empirically determined based on which value gives the best solution.

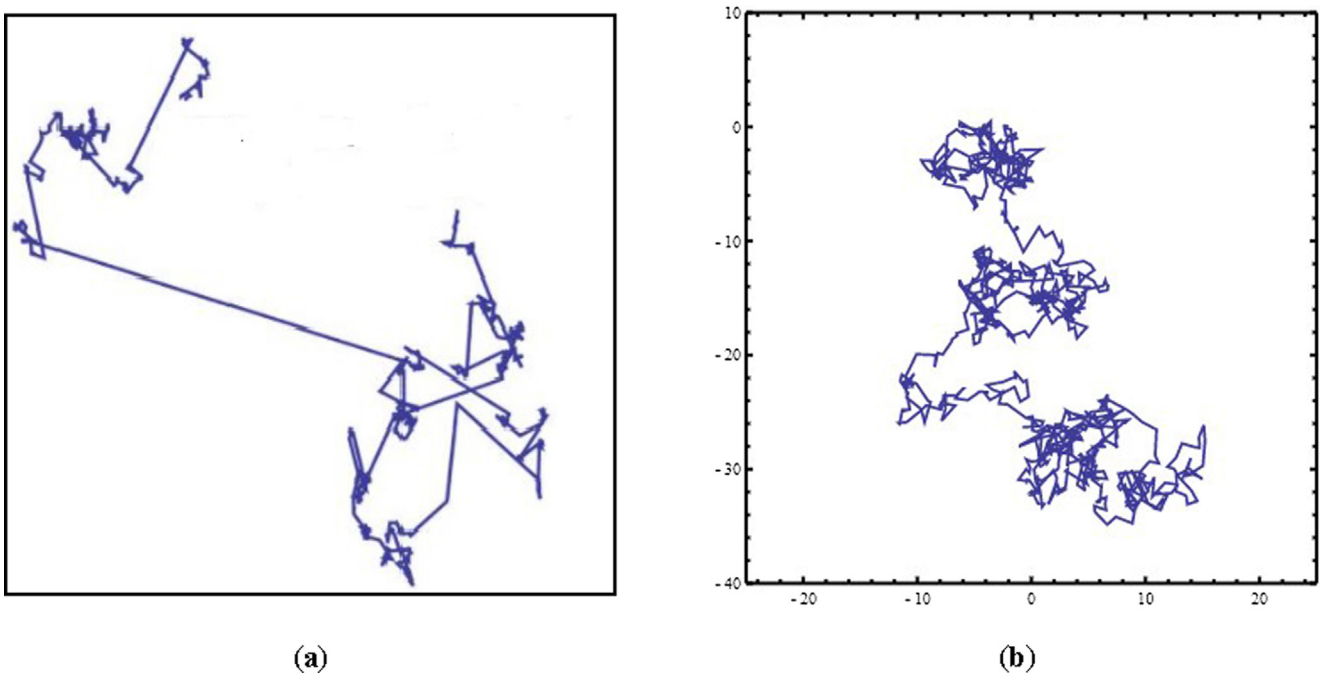


**Fig. 1.** Trajectories (a) Levy flight motion; (b) Brownian motion.

**Algorithm 1:** The basic Framework of IMPA.

```
Define system data such as; line data, bus data, generation data
Define MPA parameters: T_max, NP, Bw_min, Bw_max, b.
Initialize the populations randomly according to Eq. (32).
While T ≤ T_max do
    Calculate the objective function for the generated populations by running the power flow solution.
    Create the Elite matrix
    If T < (1/3)T_max
        Update the location of the prey according to Eq. (37).
    Else If (1/3)T_max ≤ T ≤ (2/3)T_max
        Update half of the populations according to Eq. (39).
        Update of the other half of populations according to Eq. (41).
    Else If T > (2/3)T_max
        Update the populations according to Eq. (43).
    End If
    Calculate the objective function of the updated population by running the power flow.
    Apply the Marine Memory saving
    Update the populations based on FAD's effect and Eddy formation according to Eq. (44).
    If T < (1/2)T_max
        Update the location of the prey according to Eq. (45).
    Else
        Update half of the populations according to Eq. (46) or (47).
    End if
End while
```

Finally, the proposed IMPA algorithm is based on the conventional MPA's searching capabilities by using two enhancement strategies. The proposed algorithm is implemented for solving the ORPD, one of the most important and common optimization problems. ORPD is solved at deterministic and probabilistic conditions. In deterministic condition, three objective functions are considered, including the power loss, the VD and the stability index according to equations (6), (7), and (9) with considering the system constraints which have been depicted using equations from (12) to (18). In probabilistic condition, ORPD has been solved to reduce the expected power loss (50). The uncertainty of the system is modeled by a scenario-based approach to combine the uncertainty of load, solar irradiance, and wind speed. The Pseudo-code for the improved Marian Predator is depicted in Algorithm 1. Fig. 2 also shows the steps of applying the IMPA for the ORPD solution.

## 5. Result and discussions

The simulations are performed for all given objectives to solve ORPD problems on IEEE 30-bus systems with and without RERs on MATLAB R2019b on PC Core i7 CPU @ 1.80 GHz 8 GB RAM. For

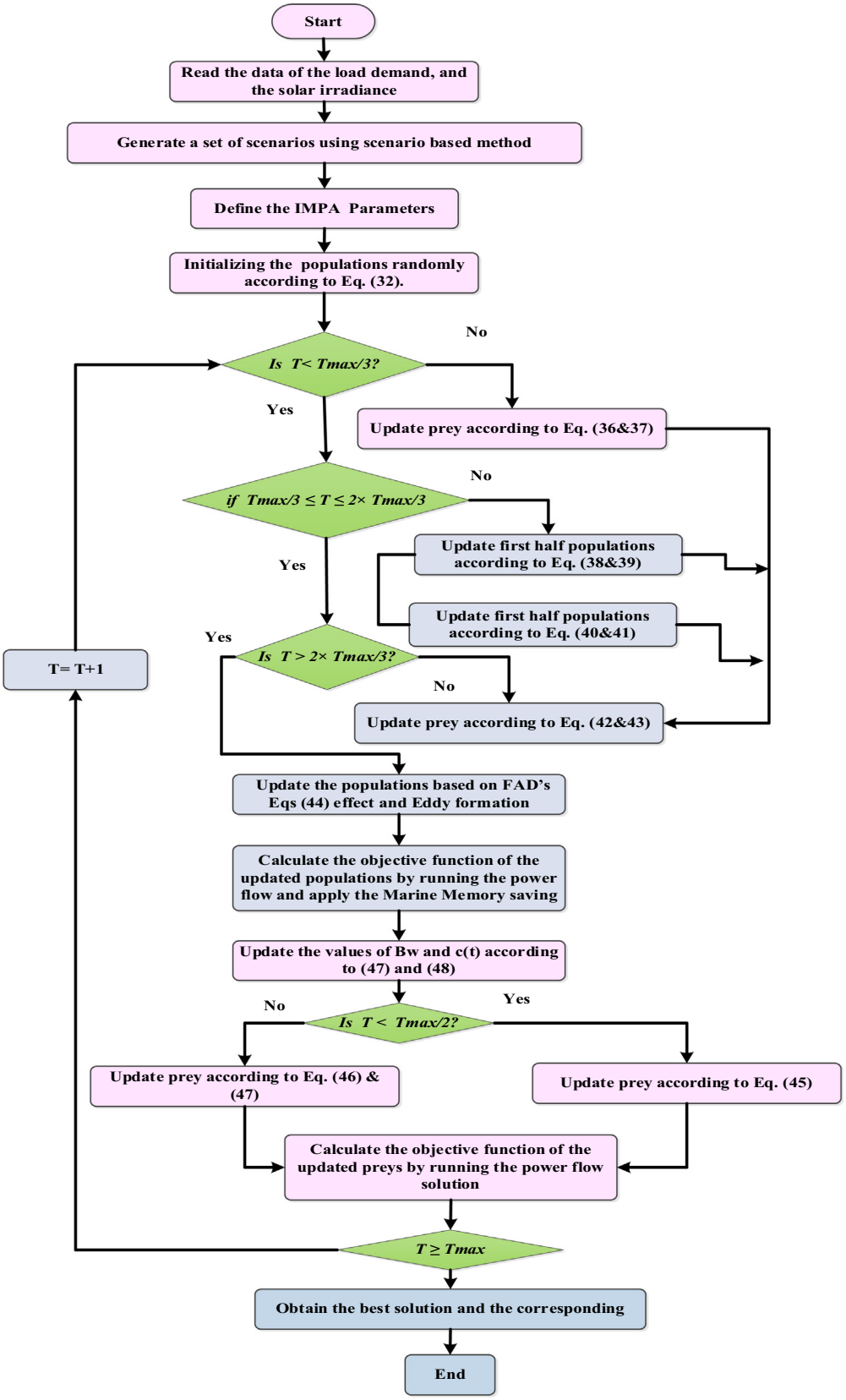


**Fig. 2.** Application of the IMPA for solving the stochastic ORPD.

all given cases, the population size, maximum number of iterations and number of trail runs are selected to be 25, 50 and 30, respectively. The IEEE 30-bus standard system consists of 6 generators, 4 transformers, 41 transmission lines, and 9 shunt Var compensators. For IEEE30 bus system using without and with RERs, the control voltages limits of the generators within range [0.95–1.1]

**Table 2**
Statistical results of MPA and IMPA for Different Considered Objective Functions (IEEE 30 BUS STANDARD).

| | Power Losses (MW) | | Voltage Deviation (p.u) | | Voltage Stability (p.u) | |
|---|---|---|---|---|---|---|
| | MPA | IMPA | MPA | IMPA | MPA | IMPA |
| Average | 4.6216 | 4.5677 | 0.1549 | 0.1250 | 0.1141 | 0.1135 |
| Best | 4.5801 | 4.5430 | 0.1380 | 0.1096 | 0.1132 | 0.1129 |
| Worst | 4.6724 | 4.6028 | 0.1807 | 0.1493 | 0.1154 | 0.1142 |
| Time (Sec) | 12.142 | 19.3487 | 12.2126 | 19.7413 | 11.9291 | 11.7932 |

**Table 3**
Optimal control variables Values for power losses, voltage deviations and voltage stability by application MPA and IMPA.

| Control Variables | Min | Max | Power Losses (MW) | | Voltage Deviation (p.u) | | Voltage Stability (p.u) | |
|---|---|---|---|---|---|---|---|---|
| | | | MPA | IMPA | MPA | IMPA | MPA | IMPA |
| | **Generator Voltages** | | | | | | | |
| V1 (p.u) | 0.9 | 1.1 | 1.100000 | 1.099996 | 1.006944 | 0.999664 | 1.096081 | 1.099749 |
| V2 (p.u) | 0.9 | 1.1 | 1.095235 | 1.094483 | 1.041686 | 0.948244 | 1.088062 | 1.099607 |
| V5 (p.u) | 0.9 | 1.1 | 1.076817 | 1.074851 | 1.011228 | 1.065047 | 1.08578 | 1.099849 |
| V8 (p.u) | 0.9 | 1.1 | 1.07877 | 1.077199 | 0.996304 | 1.038354 | 1.100000 | 1.098322 |
| V11 (p.u) | 0.9 | 1.1 | 1.099991 | 1.098760 | 1.099806 | 1.026251 | 1.097505 | 1.099941 |
| V13 (p.u) | 0.9 | 1.1 | 1.099744 | 1.100000 | 1.026884 | 1.033202 | 1.099958 | 1.099947 |
| | **Transformer Tap Ratios** | | | | | | | |
| T11 | 0.9 | 1.1 | 1.003265 | 1.034555 | 1.058206 | 0.997727 | 1.011192 | 1.021702 |
| T12 | 0.9 | 1.1 | 0.991808 | 0.904526 | 0.952344 | 0.914335 | 1.098784 | 0.929464 |
| T15 | 0.9 | 1.1 | 1.005639 | 0.980967 | 0.984524 | 1.018208 | 0.973701 | 1.010951 |
| T36 | 0.9 | 1.1 | 0.994341 | 0.983898 | 0.956384 | 0.967076 | 0.976312 | 0.987341 |
| | **Shunt VAR Compensators** | | | | | | | |
| Q10 (p.u) | 0 | 0.05 | 0.003728 | 0.448733 | 0.407815 | 0.109906 | 0.49999 | 0.494074 |
| Q12 (p.u) | 0 | 0.05 | 0.125029 | 0.498782 | 0.306809 | 0.026837 | 0.495167 | 0.497984 |
| Q15 (p.u) | 0 | 0.05 | 0.406421 | 0.066142 | 0.133845 | 0.495746 | 0.499992 | 0.468622 |
| Q17 (p.u) | 0 | 0.05 | 0.294272 | 0.385893 | 0.267874 | 0.000472 | 0.494656 | 0.498651 |
| Q20 (p.u) | 0 | 0.05 | 0.487133 | 0.499977 | 0.343778 | 0.500000 | 0.499942 | 0.487517 |
| Q21 (p.u) | 0 | 0.05 | 0.466238 | 0.499696 | 0.103920 | 0.297825 | 0.499985 | 0.500000 |
| Q23 (p.u) | 0 | 0.05 | 0.203727 | 0.468633 | 0.157127 | 0.498606 | 0.495253 | 0.496884 |
| Q24 (p.u) | 0 | 0.05 | 0.461544 | 0.497548 | 0.499220 | 0.287937 | 0.497917 | 0.495558 |
| Q29 (p.u) | 0 | 0.05 | 0.497379 | 0.452891 | 0.173972 | 0.490328 | 0.498188 | 0.494459 |
| | Objective Functions | | | | | | | |
| Objectives | | | **4.5801 MW** | **4.5430 MW** | **0.1380p.u** | **0.1096p.u** | **0.1132p.u** | **0.1129p.u** |
| Reduction in % | | | 21.18 % | 21.82 % | 84.12 % | 87.34 % | 34.30 % | 34.47 % |

p.u., the transformers tap settings within the range [0.9–1.1] and output reactive powers of Var compensators are varied within the range [0–0.5] p.u. The detailed system data are given in [64]. The system's active and reactive load demands are considered 283.2 MW and 126.2 MVAr, respectively [65].

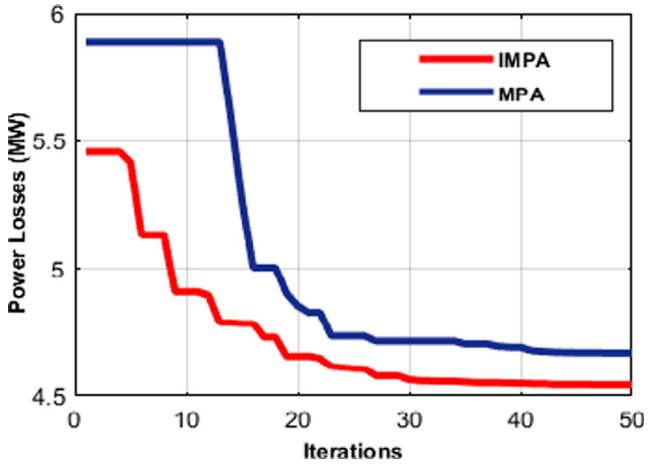


**Fig. 3.** The convergence characteristics of Power Losses (MW) using MPA and IMPA for power loss.

There are three study cases are presented for ORPD solutions without and with RERs integration; the details of the study cases are given below:

- Case A: Optimal Reactive Power Dispatch Without Integration of RERs (IEEE 30)
- Case B: Optimal Reactive Power Dispatch with Integration of RERs (IEEE 30)

### *5.1. Case A: Optimal reactive power Dispatch without integration of RERs (IEEE 30)*

In the case of A, the ORPD problem is solved without considering RERs by application of the MPA and the IMPA. The considered objective functions are transmission losses reduction, voltage deviations reduction enhancement of the voltage stability. In the initial case, the power loss is 5.811 MW [1], summation of the voltage deviations is 0.8691p.u. [46] and the voltage stability index is 0.1723p.u. [32]. To demonstrate the best performance that achieved by the proposed IMPA algorithm, the results are compared to the initial case, the standard MPA and those obtained by other techniques.

#### *5.1.1. Minimization of power losses*

The simulations are performed between the IMPA and traditional MPA in order to minimize power losses. The worst, best, average values, as well as simulation time of both algorithms, are reported in Table 2.

From the statistical results of Table 2, the IMPA is better than the standard MPA for power loss reduction. Table 3 shows the best control variables obtained by applying the IMPA and the traditional MPA. Judging from Table 3, the best value of IMPA is 4.5430 MW which is 0.81% less than the traditional MPA. Fig. 3 illustrates the best and convergence response achieved by IMPA algorithm over traditional MPA where the power losses are converged at 42th iteration by application MPA while it is converged at 38th iteration by application of the IMPA.

In addition, Table 4 signified the results of different *meta*-heuristic techniques to solve ORPD problem, where the IMPA reported its efficient performance with the reduction of power losses to 21.82 % in comparison with Sine-cosine Algorithm (SCA), Quasi-oppositional Teaching Learning-based Optimization (QOTLBO), Particle Swarm Optimization and Grey-wolf Optimization (PSOGWO), Firefly Algorithm and the Adaptive Particularly Tunable Fuzzy Particle Swarm Optimization (FA-APTFPSO-IV), Self-balanced Differential Evolution (SBDE), Jaya Algorithm (JA), Harmony Search Algorithm (HAS), Whale Optimization Algorithm (WOA), Tabu Search (TS), Artificial Bee Colony (ABC), Improved Marine Predators Algorithm and Particle Swarm Optimization (IMPAPSO), Differential Evolution (DE) and Firefly Algorithm (FA), respectively. The overall results indicated the efficiency of the proposed IMPA.

### 5.1.2. Minimization of voltage Deviation

In this case, the objective is to minimize the voltage deviations using IMPA and traditional MPA. The best average, worst and the simulation time are given in Table 2. Referring to Table 2, the obtained results obtained by IMPA are better than those obtained by applying the traditional MPA. The optimal control variables for this case obtained by application the MPA and the IMPA are listed in the 6th and 7th columns of Table 3, respectively. The minimum *VD* that obtained by IMPA is 0.1096p.u which is less by 20.58% compared with MPA. Moreover, to validate the efficiency of IMPA, the results are compared to different *meta*-heuristic optimization techniques given in Table 5.

The overall results demonstrated that the proposed IMPA is reduced the voltage deviations to 87.34 % and the reduction percentage is less than the reported algorithms in Table 5, such as; Self-organizing Hierarchical Particle Swarm Optimization with Time-varying Acceleration Coefficients (SPSO-TVAC), Stochastic Weight Tradeoff Particle Swarm Optimization (SWT-PSO), Symbiotic Organisms Search (SSO), Ant Lion Optimizer (ALO), pseudo-gradient Particle Swarm Optimization (PG-PSO), Improved Marine Predators Algorithm and Particle Swarm Optimization (IMPAPSO), Genetic Particle Swarm Optimization Algorithm with Symbiotic Organisms Search (HGPSOS), Gravitational Search Algorithm and Conditional Selection Strategies (GSA-CSS), Particle Swarm Optimization and Time-varying Acceleration (PSO-TVA), Particle Swarm Optimization with Constriction Factor (PSO-CF), Gravita-

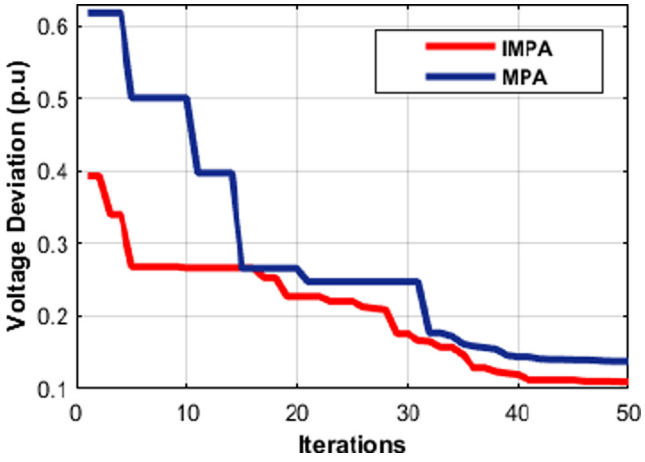


**Fig. 4.** The convergence characteristics of Voltage Deviation (p.u) using MPA and IMPA.

**Table 4**
A Comparison of Power Losses by Application of Different Algorithms.

| Algorithm | Plosses (MW) | Reduction % | Algorithm | Plosses (MW) | Reduction % |
|---|---|---|---|---|---|
| SCA [10] | 4.5538 | 21.63 | TS [56] | 4.9203 | 15.32 |
| QOTLBO [24] | 4.5594 | 21.54 | WOA [53] | 4.5943 | 20.40 |
| PSOGWO [52] | 5.09037 | 12.40 | ABC [14] | 5.790 | 0.36 |
| FA-APTFPSO-IV [48] | 4.8664 | 16.25 | IMPAPSO [55] | 5.07510941 | 15.57 |
| SBDE [51] | 4.590 | 21.01 | DE [50] | 4.5550 | 21.61 |
| JA [49] | 4.625 | 20.93 | FA [57] | 4.5691 | 21.37 |
| HSA [54] | 4.9059 | 12.66 | TS [56] | 4.9203 | 15.32 |

**Table 5**
A Comparison of Voltage Deviation by Application of Different Algorithms.

| Algorithm | $VD(p.u)$ | Reduction % | Algorithm | $VD(p.u)$ | Reduction % |
|---|---|---|---|---|---|
| SPSO-TVAC [58] | 0.1354 | 84.42 | HGPSOS [61] | 0.1179 | 86.43 |
| SWT-PSO [58] | 0.1614 | 81.42 | GSA-CSS [62] | 0.12394 | 85.73 |
| SSO [60] | 0.19304 | 77.78 | PSO-TVA [58] | 0.2064 | 76.25 |
| ALO [59] | 0.1192 | 86.28 | PSO-CF [58] | 0.1287 | 85.19 |
| PG-PSO [58] | 0.1202 | 86.16 | GSA [62] | 0.17241 | 80.16 |
| SWT-PSO [58] | 0.1614 | 81.42 | PSO [62] | 0.10462 | 87.96 |
| IMPAPSO [55] | 0.2487 | 71.38 | AEFA [34] | 0.1313 | 84.89 |
| SPSO-TVAC [58] | 0.1354 | 84.42 | | | |

**Table 6**
A Comparison of Voltage Stability Enhancement by Application of Different Algorithms.

| Algorithm | $L_{max}(p.u)$ | Reduction % | Algorithm | $L_{max}(p.u)$ | Reduction % |
|---|---|---|---|---|---|
| HGPSOS [61] | 0.1315 | 23.67 | DE [50] | 0.1246 | 27.68 |
| APOPSO [61] | 0.1377 | 20.08 | GSA [61] | 0.1349 | 21.70 |
| APO [63] | 0.1239 | 28.09 | ALO [59] | 0.1253 | 27.27 |
| IALO [59] | 0.1246 | 27.68 | | | |

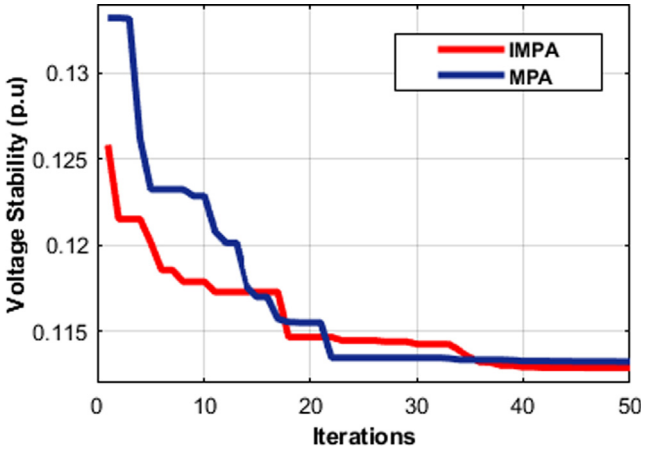


**Fig. 5.** The convergence characteristics of Voltage Stability (p.u) using MPA and IMPA.

tional Search Algorithm (GSA), Particle Swarm Optimization (PSO) and Artificial Electric Field Algorithm (AEFA), respectively. Fig. 4 demonstrates the best convergence performance achieved by the proposed IMPA. However, The VD is converged at 44th and 42th by application of the MPA and the IMPA; respectively, the obtained results by the IMPA are better than those obtained by MPA.

*5.1.3. Enhancement of the voltage stability index*

The third objective is to enhance the voltage stability for which the simulations are carried out using the proposed IMPA and traditional MPA. The outcomes of both algorithms are mentioned in Table 2, where the voltage stability value of IMPA is 0.1129p.u. which is 0.26% less reported to the traditional MPA. The optimal control variables obtained by applying the MPA and the IMPA techniques for voltage stability enhancement are depicted in the 8th and 9th columns of Table 3.

A comparison between the proposed IMPA technique and other algorithms for this case are depicted in Table 6. Judging from Table 6, the outputs of the proposed IMPA are compared to the base case and other *meta*-heuristic techniques, which is at the highest values of reduction to 34.47 % more than the reported algorithms such as; Hybrid Genetic Particle Swarm Optimization Algorithm with Symbiotic Organisms Search (HGPSOS), Particle swarm Optimization and Artificial Physics Optimization (APOPSO), Artificial Physics Optimization (APO), Improved Ant Lion Optimization (IALO), Differential Evolution (DE), Gravitational Search Algorithm (GSA) and Ant Lion Optimization (ALO), respectively. Fig. 5 illustrates the best convergence response achieved by the proposed

**Table 7**
The Generated Scenarios of Load Demand, Solar Irradiation, Wind Speed with their Corresponding Probabilities.

| Scenario | Loading % | Solar Irradiance (W/m$^2$) | Wind Speed (m/s) | $\tau_{d,\,i}$ | $\tau_{\,Solar,\,m}$ | $\tau_{\,wind,\,k}$ | $\tau_S$ |
|---|---|---|---|---|---|---|---|
| S1 | 58.5892 | 691.4611 | 5.3953 | 0.3085 | 0.1255 | 0.6321 | 0.01851 |
| S2 | 58.5892 | 691.4611 | 11.1082 | 0.3085 | 0.1255 | 0.2789 | 0.009255 |
| S3 | 58.5892 | 691.4611 | 16.4918 | 0.3085 | 0.1255 | 0.0889 | 0.003085 |
| S4 | 58.5892 | 857.2083 | 5.3953 | 0.3085 | 0.1671 | 0.6321 | 0.03702 |
| S5 | 58.5892 | 857.2083 | 11.1082 | 0.3085 | 0.1671 | 0.2789 | 0.01851 |
| S6 | 58.5892 | 857.2083 | 16.4918 | 0.3085 | 0.1671 | 0.0889 | 0.00617 |
| S7 | 58.5892 | 970.6447 | 5.3953 | 0.3085 | 0.7075 | 0.6321 | 0.12957 |
| S8 | 58.5892 | 970.6447 | 11.1082 | 0.3085 | 0.7075 | 0.2789 | 0.064785 |
| S9 | 58.5892 | 970.6447 | 16.4918 | 0.3085 | 0.7075 | 0.0889 | 0.021595 |
| S10 | 72.0663 | 691.4611 | 5.3953 | 0.5328 | 0.1255 | 0.6321 | 0.031968 |
| S11 | 72.0663 | 691.4611 | 11.1082 | 0.5328 | 0.1255 | 0.2789 | 0.015984 |
| S12 | 72.0663 | 691.4611 | 16.4918 | 0.5328 | 0.1255 | 0.0889 | 0.005328 |
| S13 | 72.0663 | 857.2083 | 5.3953 | 0.5328 | 0.1671 | 0.6321 | 0.063936 |
| S14 | 72.0663 | 857.2083 | 11.1082 | 0.5328 | 0.1671 | 0.2789 | 0.031968 |
| S15 | 72.0663 | 857.2083 | 16.4918 | 0.5328 | 0.1671 | 0.0889 | 0.010656 |
| S16 | 72.0663 | 970.6447 | 5.3953 | 0.5328 | 0.7075 | 0.6321 | 0.223776 |
| S17 | 72.0663 | 970.6447 | 11.1082 | 0.5328 | 0.7075 | 0.2789 | 0.111888 |
| S18 | 72.0663 | 970.6447 | 16.4918 | 0.5328 | 0.7075 | 0.0889 | 0.037296 |
| S19 | 85.2514 | 691.4611 | 5.3953 | 0.1587 | 0.1255 | 0.6321 | 0.009522 |
| S20 | 85.2514 | 691.4611 | 11.1082 | 0.1587 | 0.1255 | 0.2789 | 0.004761 |
| S21 | 85.2514 | 691.4611 | 16.4918 | 0.1587 | 0.1255 | 0.0889 | 0.001587 |
| S22 | 85.2514 | 857.2083 | 5.3953 | 0.1587 | 0.1671 | 0.6321 | 0.019044 |
| S23 | 85.2514 | 857.2083 | 11.1082 | 0.1587 | 0.1671 | 0.2789 | 0.009522 |
| S24 | 85.2514 | 857.2083 | 16.4918 | 0.1587 | 0.1671 | 0.0889 | 0.003174 |
| S25 | 85.2514 | 970.6447 | 5.3953 | 0.1587 | 0.7075 | 0.6321 | 0.066654 |
| S26 | 85.2514 | 970.6447 | 11.1082 | 0.1587 | 0.7075 | 0.2789 | 0.033327 |
| S27 | 85.2514 | 970.6447 | 16.4918 | 0.1587 | 0.7075 | 0.0889 | 0.011109 |

**Table 8**
Selected Scenarios and the Corresponding Output Powers of Renewable Systems and The Expected Power Losses.

| Scenario | Output Power of RERs (PV + Wind) | | MPA | IMPA | MPA | IMPA |
|---|---|---|---|---|---|---|
| | $P_s(MW)$ | $P_w(MW)$ | $P_{Loss}(MW)$ | $P_{Loss}(MW)$ | $EPL(MW)$ | $EPL(MW)$ |
| S1 | 34.5731 | 13.8190 | 1.7233 | 1.3828 | 0.0319 | 0.0256 |
| S2 | 34.5731 | 46.7781 | 1.7486 | 0.9973 | 0.0162 | 0.0092 |
| S3 | 34.5731 | 75.0000 | 2.8075 | 1.4348 | 0.0087 | 0.0044 |
| S4 | 42.8604 | 13.8190 | 1.7397 | 1.4273 | 0.0644 | 0.0528 |
| S5 | 42.8604 | 46.7781 | 1.334 | 1.1348 | 0.0247 | 0.0210 |
| S6 | 42.8604 | 75.0000 | 1.8374 | 1.4962 | 0.0113 | 0.0092 |
| S7 | 48.5322 | 13.8190 | 1.5680 | 1.3499 | 0.2032 | 0.1749 |
| S8 | 48.5322 | 46.7781 | 1.5510 | 1.0420 | 0.1005 | 0.0675 |
| S9 | 48.5322 | 75.0000 | 2.1840 | 1.5182 | 0.0472 | 0.0328 |
| S10 | 34.5731 | 13.8190 | 3.0660 | 2.3495 | 0.0980 | 0.0751 |
| S11 | 34.5731 | 46.7781 | 1.5935 | 1.4536 | 0.0255 | 0.0232 |
| S12 | 34.5731 | 75.0000 | 1.6190 | 1.2587 | 0.0086 | 0.0067 |
| S13 | 42.8604 | 13.8190 | 2.9748 | 2.1922 | 0.1902 | 0.1402 |
| S14 | 42.8604 | 46.7781 | 1.7095 | 1.3033 | 0.0546 | 0.0417 |
| S15 | 42.8604 | 75.0000 | 1.5964 | 1.3104 | 0.0170 | 0.0140 |
| S16 | 48.5322 | 13.8190 | 2.5309 | 2.0957 | 0.5663 | 0.4690 |
| S17 | 48.5322 | 46.7781 | 1.4970 | 1.2995 | 0.1675 | 0.1454 |
| S18 | 48.5322 | 75.0000 | 1.5216 | 1.2399 | 0.0567 | 0.0462 |
| S19 | 34.5731 | 13.8190 | 5.7422 | 4.2806 | 0.0547 | 0.0408 |
| S20 | 34.5731 | 46.7781 | 3.3229 | 2.5349 | 0.0158 | 0.0121 |
| S21 | 34.5731 | 75.0000 | 1.9961 | 1.7790 | 0.0032 | 0.0028 |
| S22 | 42.8604 | 13.8190 | 5.5598 | 3.8647 | 0.1059 | 0.0736 |
| S23 | 42.8604 | 46.7781 | 2.7496 | 2.5376 | 0.0262 | 0.0242 |
| S24 | 42.8604 | 75.0000 | 1.9498 | 1.7617 | 0.0062 | 0.0056 |
| S25 | 48.5322 | 13.8190 | 4.4727 | 3.5586 | 0.2981 | 0.2372 |
| S26 | 48.5322 | 46.7781 | 2.5271 | 2.1273 | 0.0842 | 0.0709 |
| S27 | 48.5322 | 75.0000 | 1.9031 | 1.5764 | 0.0211 | 0.0175 |
| **TEPL (MW)** | | | | | **2.3079** | **1.8436** |

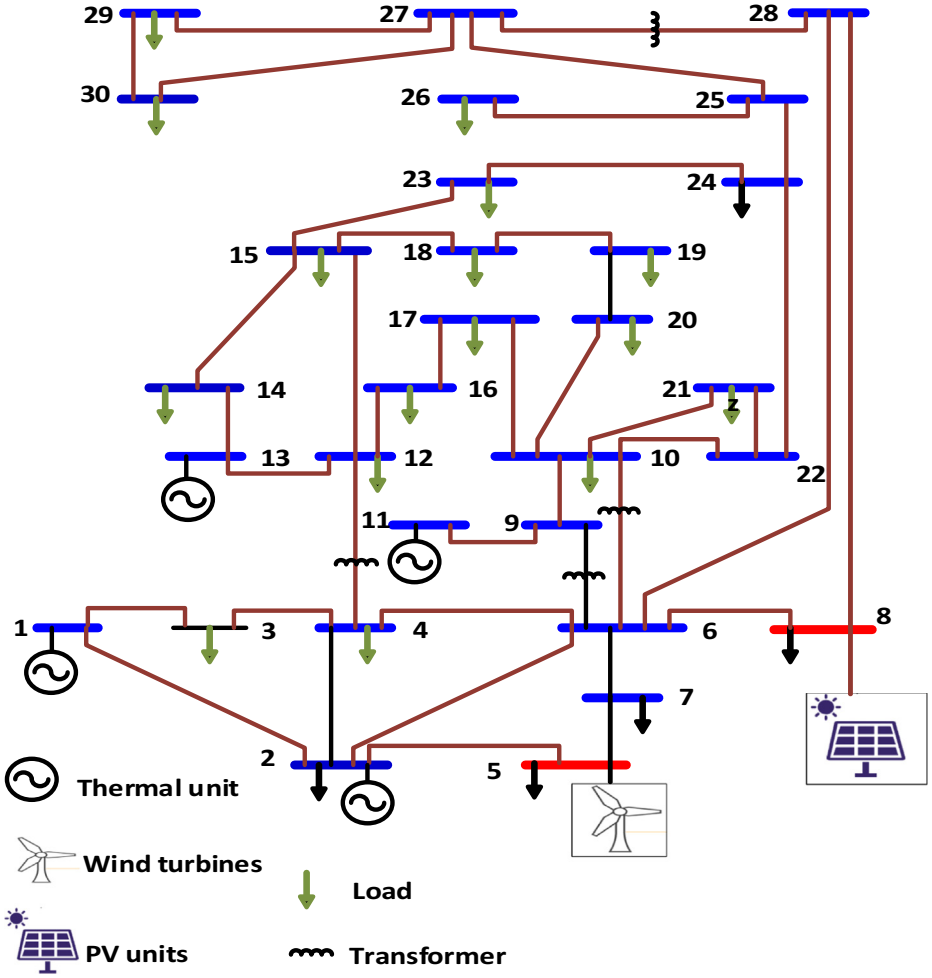


**Fig. 6.** The single line diagram of the modified IEEE 30-bus system with Integration of RERs.

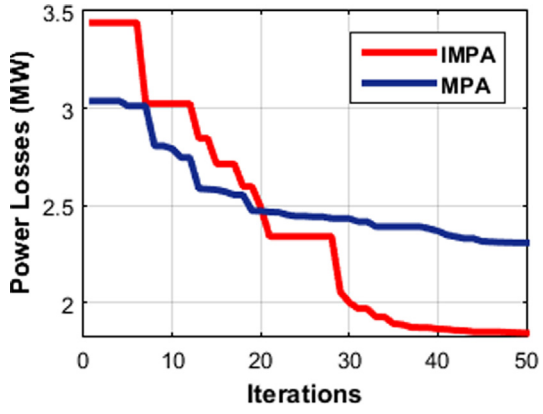


**Fig. 7.** The convergence characteristics of Power Losses (p.u) using MPA and IMPA considering RERs.

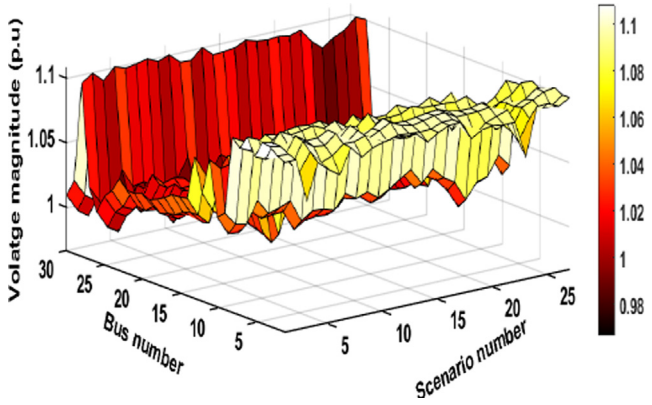


**Fig. 8.** The system voltage profile for generated scenarios by application the IMPA.

IMPA. From Fig. 5, it is clear that the stability index is converged at 22th and 36th by application of the MPA and the IMPA, respectively. However, the obtained results by IMPA are better than those obtained by application of the MPA. Judging from Table 6, the outputs of the proposed IMPA are compared to the base case and other *meta*-heuristic techniques, which is at the highest values of reduction to 34.47 % more than the reported algorithms such as; HGPSOS, APOPSO, APO, IALO, DE, GSA and ALO, respectively.

### *5.2. Case B: Optimal reactive power Dispatch wit integration of renewable energy resources*

In this case, the ORPD is solved in the presence of renewable energy resources. The IEEE 30-bus system is modified by incorporating the wind and solar generator units at 5 and 8 buses, receptively as depicted in Fig. 6.

Due to the stochastic nature of RERs, the uncertainty of solar and wind are considered as well as the uncertainties of the load demands. A 75 MW windfarm is connected to bus 5, which consisting 25 turbines of 3 MW rated power. Each connected turbine in windfarm has cut-in, cut-out and the rated speed are 3, 25 and 16 m/s, respectively. Whereas the 50 MW PV system is connected at bus 8 and its solar irradiance is considered 1000 W/m2 [32].

The three individual scenarios with their probabilities to model the uncertainty of wind speed, solar irradiance and load demands are given in Table 1. To combine these uncertainties, the total number of scenarios will be 27 using Eq. (31), and the detail of these scenarios are given in Table 7. The aim of solving the OPRD problem is to minimize the expected power losses under uncertainty which can be formulated as follows:

$$TEPL = \sum_{r=1}^{N_{GS}} EPL_r = \sum_{r=1}^{N_{GS}} \tau_{S,r} \times P_{Losses,r} \tag{50}$$

where $TEPL$ is the total expected losses, $EPL_r$ presents the expected power losses for $r^{th}$ scenario while $N_{GS}$ is the number of generated scenarios. The total expected power losses without considering RERs are 5.2456 MW, while after incorporating solar and wind power into the system, the $TEPL$ with the application of the MPA and the IMPA values are 1.8436 MW and 2.3079 MW, respectively. In other words, the percentage reductions of the expected power losses by applying the MPA and the IMPA are reported to 56.00 % and 64.85%, respectively.

Table 8 shows the outpower power of wind turbine and PV generation systems as well as the corresponding power losses and the probabilities of different scenarios with the application of the MPA and the IMPA. It is clear that the power losses are varied with the output powers of the RER. Fig. 7 illustrates the best convergence response achieved by the proposed IMPA compared to traditional MPA. From Fig. 7, it is clear to mention that the power losses are converged at 42th and 33th by application of the MPA and the IMPA, respectively. Fig. 8 shows the voltage profile for each scenario for the IEEE 30-bus system. It is obvious that the voltages are within their allowable limits.

Fig. 9(a), (b) and (c) illustrate the optimal values of the control variables, including the voltages of at each generation buses, transformer taps and the injected reactive powers by compensation units which IMPA has obtained. It is clear that the settings of the control variables have different values for each scenario.

It should be highlighted here that to evaluate the proposed improvement, Figs. 3, 4, 5, 7 and 8 give the convergence curves of the considered objective functions. According to these figures, the IMPA has fast convergance charactristics at the beginning of search, indicating that the good search regions can be obtained due to the proposed explotation process.

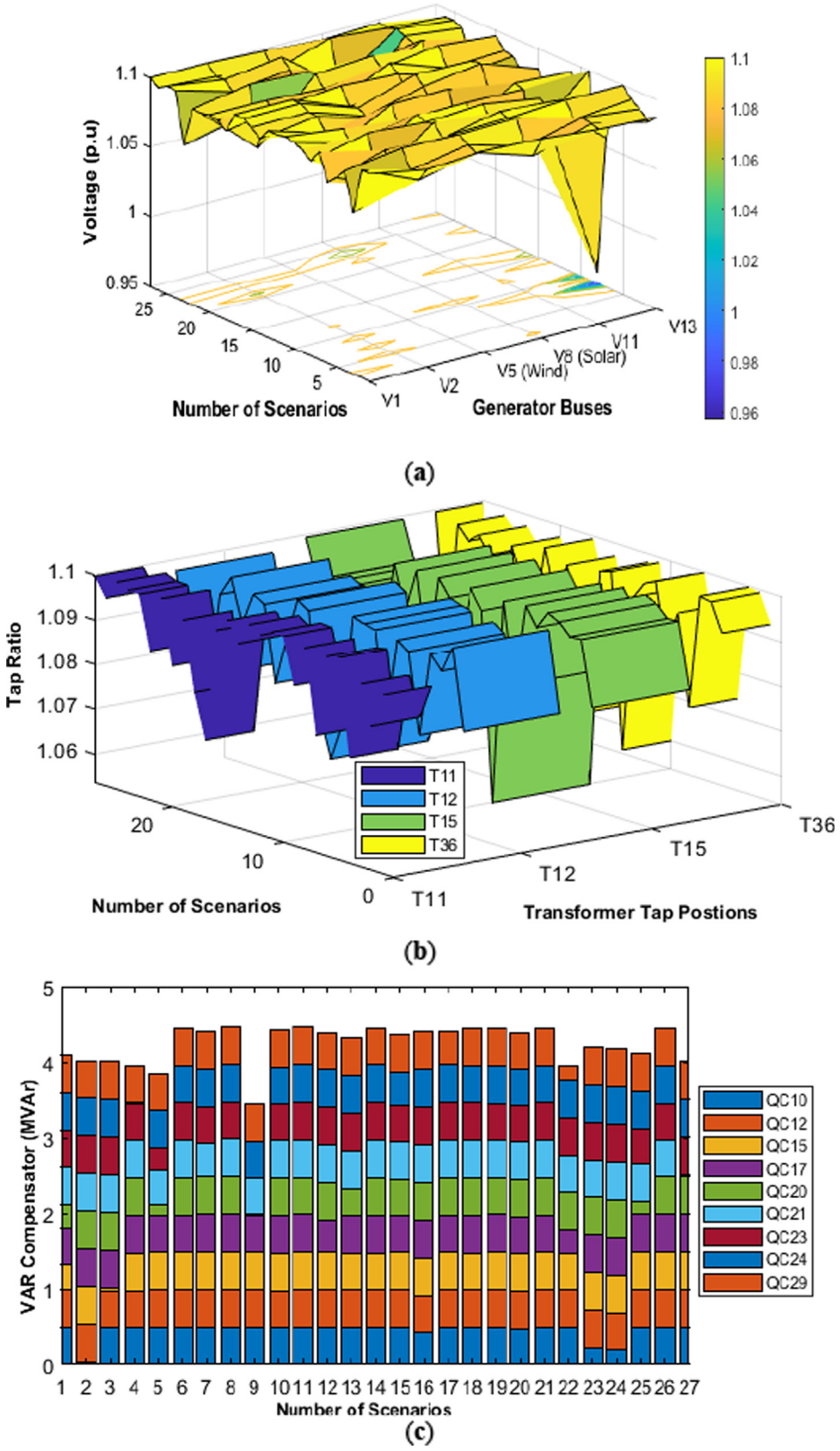


**Fig. 9.** The optimal values for studied scenarios of (a) the voltages at the generation buses, (**b**) the VAR compensators for the generated scenarios, (**c**) The injected VAR in MVAr.

## 6. Conclusion

In this research, an Improved Marine Predators Algorithm (IMPA) is efficiently applied to solve the ORPD problem with and without considering RERs to minimize the power losses, voltage deviations, and enhance the voltage stability. The modification in IMPA is based on updating the positions of the predators in a spiral path around the sorted elite predators, while in the final iterative process, the positions of the predators are updated close to the best predator in adaptive steps. The proposed algorithm has been successfully implemented for solving the ORPD on IEEE 30-bus and the outcomes have been compared with the traditional MPA and other reported techniques.

In addition, ORPD has been solved with the integration of wind and PV systems considering the uncertainties of three parameters, including wind speed, solar irradiation, and load demands. The uncertainty models of these parameters are represented by Weibull PDF, Beta PDF and normal PDF, respectively. Then, the scenario-based model has been employed to combine the uncertainties of these parameters where a set of scenarios have been generated due to the combination of these parameters. The simulation results verified the superiority of the proposed algorithm compared with the traditional MPA and the other reported algorithms for solving the ORPD. In addition, the reduction in expected power losses is achieved 64.85% by integrating the RERs into the system using IMPA.

## Declaration of Competing Interest

The authors declare that they have no known competing financial interests or personal relationships that could have appeared to influence the work reported in this paper.

## Acknowledgements

The author (Hossam M. Zawbaa) thanks the European Union's Horizon 2020 research and Enterprise Ireland for their support under the Marie Skłodowska-Curie grant agreement No. 847402. The authors thank the support of the National Research and Development Agency of Chile (ANID), ANID/Fondap/15110019.

## References

[1] Khan NH, Wang Y, Tian D, Raja MAZ, Jamal R, Muhammad Y. Design of fractional particle swarm optimization gravitational search algorithm for optimal reactive power dispatch problems. IEEE Access 2020;8:146785–806.
[2] Jamal R, Men B, Khan NH, Raja MAZ. Hybrid bio-inspired computational heuristic paradigm for integrated load dispatch problems involving stochastic wind. Energies 2019;12(13):2568.
[3] Granville S. Optimal reactive dispatch through interior point methods. IEEE Trans Power Syst 1994;9(1):136–46.
[4] Terra LDB, Short MJ. Security-constrained reactive power dispatch. IEEE Trans Power Syst 1991;6(1):109–17.
[5] Lee K, Park Y, Ortiz J. A United Approach to Optimal Real and Reactive Power Dispatch. IEEE Trans. on Power Apparatus and Syst. 1985;PAS-104 (5):1147–53.
[6] Quintana VH, Santos-Nieto M. Reactive-power dispatch by successive quadratic programming. IEEE Trans Energy Convers 1989;4(3):425–35.
[7] Jan RM, Chen N. Application of the fast Newton-Raphson economic dispatch and reactive power/voltage dispatch by sensitivity factors to optimal power flow. IEEE Trans Energy Convers 1995;10(2):293–301.
[8] Alabd S, Sulaiman MH, Rashid MIM. Optimal Power Flow Solutions for Power System Operations Using Moth-Flame Optimization Algorithm. In: Proceedings of the 11th National Technical Seminar on Unmanned System Technology 2019. Springer 2021, 207-219. https://doi.org/10.1007/978-981-15-5281-6_15
[9] El-Desouki H, El-Zonkoly A, Aly G. Optimal Active and Reactive Power Dispatch and Excitation System Controller Design Using Genetic, Algorithm. (Dept. E). Mansoura Eng J 2021;28(2):1–16.
[10] Saddique MS, Bhatti AR, Haroon SS, Sattar MK, Amin S, Sajjad IA, et al. Solution to optimal reactive power dispatch in transmission system using meta-heuristic techniques–Status and technological review. Electr Power Syst Res 2020;178:106031. doi: https://doi.org/10.1016/j.epsr.2019.106031.
[11] Jamal R, Men B, Khan NH. A novel nature inspired meta-heuristic optimization approach of GWO optimizer for optimal reactive power dispatch problems. IEEE Access 2020;8:202596–610.
[12] Sulaiman MH, Mustaffa Z, Saari MM, Daniyal H. Barnacles mating optimizer: a new bio-inspired algorithm for solving engineering optimization problems. Eng Appl Artif Intell 2020;87:103330. doi: https://doi.org/10.1016/j.engappai.2019.103330.
[13] Bhongade S, Tomar A, Goigowal SR. Minimization of Optimal Reactive Power Dispatch Problem using BAT Algorithm. In: 2020 IEEE First International Conference on Smart Technologies for Power, Energy and Control (STPEC) 2020, 1-5. DOI:10.1109/STPEC49749.2020.9297806
[14] Ettappan M, Vimala V, Ramesh S, Kesavan VT. Optimal reactive power dispatch for real power loss minimization and voltage stability enhancement using Artificial Bee Colony Algorithm. Microprocess Microsyst 2020;76:103085. doi: https://doi.org/10.1016/j.micpro.2020.103085.
[15] Das T, Roy R, Mandal KK, Mondal S, Mondal S, Hait P, et al. Optimal reactive power dispatch incorporating solar power using Jaya algorithm. In: Computational advancement in communication circuits and systems. Springer; 2020. p. 37–48. doi: https://doi.org/10.1007/978-981-13-8687-9_4.
[16] Htay TT, Mon KK, Lin OZ. Optimal reactive power dispatch using particle swarm optimization algorithm for Yangon distribution network. In: IOP Conference Series: Earth and Environmental Science (IOP Publishing) 2020, 463, 012152.
[17] Zand M, Chamorro HR, Nasab MA, Hosseinian SH. Optimal reactive power dispatch using θ-social mimic optimization (θ-SMO). J Intell Fuzzy Syst 2020:1–15. doi: https://doi.org/10.3233/jifs-201667.
[18] Lenin K. Bamboo Plant Intellect Deeds Optimization Algorithm for Solving Optimal Reactive Power Problem. In: In Proceedings of the 7th International Conference on Advances in Energy Research. Springer; 2021. p. 665–72. doi: https://doi.org/10.1007/978-981-15-5955-6_62.
[19] Lenin K. Levy Flight-Based White Wolf Algorithm for Solving Optimal Reactive Power Problem. In: In Advances in Communication and Computational Technology. Springer; 2021. p. 647–54.
[20] Rana N, Abd Latiff MS, Chiroma H. Whale optimization algorithm: a systematic review of contemporary applications, modifications and developments. Neural Comput Appl 2020;32:1–33.
[21] Mouassa S, Bouktir T, Salhi A. Ant lion optimizer for solving optimal reactive power dispatch problem in power systems. Eng Sci Technol Int J 2017;20 (3):885–95. doi: https://doi.org/10.1016/j.jestch.2017.03.006.
[22] Shaheen AM, El-Sehiemy RA, Farrag SM. A novel framework for power loss minimization by modified wind driven optimization algorithm. In: In 2018 International Conference on Innovative Trends in Computer Engineering (ITCE). IEEE; 2018. p. 344–9.
[23] Sakr WS, El-Sehiemy RA, Azmy AM. Adaptive differential evolution algorithm for efficient reactive power management. Appl Soft Comput 2017;53:336–51.
[24] Mandal B, Roy PK. Optimal reactive power dispatch using quasi-oppositional teaching learning-based optimization. Int J Electr Power Energy Syst 2013;53:123–34.
[25] Bhattacharya A, Chattopadhyay PK. Solving complex economic load dispatch problems using biogeography-based optimization. Expert Syst Appl 2010;37 (5):3605–15.
[26] Gafar MG, El-Sehiemy RA, Hasanien HM. A novel hybrid fuzzy-JAYA optimization algorithm for efficient ORPD solution. IEEE Access 2019;7:182078–88.
[27] Shargh S, Mohammadi-Ivatloo B, Seyedi H, Abapour M. Probabilistic multiobjective optimal power flow considering correlated wind power and load uncertainties. Renewable Energy 2016;94:10–21.
[28] Aien M, Rashidinejad M, Fotuhi-Firuzabad M. On possibilistic and probabilistic uncertainty assessment of power flow problem: A review and a new approach. Renew Sustain Energy Rev 2014;37:883–95.
[29] Moore RE, Kearfott RB, Michael JCloud. Introduction to interval analysis. Philadelphia, USA: SIAM; 2009.
[30] Karuppiah R, Martín M, Grossmann IE. A simple heuristic for reducing the number of scenarios in two-stage stochastic programming. Comput Chem Eng 2010;34(8):1246–55.
[31] Nazari-Heris M, Mohammadi-Ivatloo B. Application of robust optimization method to power system problems. Classical and recent aspects of power system optimization 2018:19–32.
[32] Khan NH, Wang Y, Tian D, Jamal R, Ebeed M, Deng Q. Fractional PSOGSA Algorithm Approach to Solve Optimal Reactive Power Dispatch Problems With Uncertainty of Renewable Energy Resources. IEEE Access 2020;8:215399–413.
[33] Abdel-Fatah S, Ebeed M, Kamel S, Nasrat L. Moth swarm algorithm for reactive power dispatch considering stochastic nature of renewable energy generation and load. In: 2019 21st International Middle East Power Systems Conference (MEPCON). IEEE 2019, 594-599.
[34] Hassan MH, Kamel S, El-Dabah MA, Khurshaid T, Dominguez-Garcia JL. Optimal reactive power dispatch with time-varying demand and renewable energy uncertainty using Rao-3 algorithm. IEEE Access 2021;9:23264–83. doi: https://doi.org/10.1109/ACCESS.2021.3056423.
[35] Biswas PP, Suganthan PN, Mallipeddi R, Amaratunga GA. Optimal reactive power dispatch with uncertainties in load demand and renewable energy sources adopting scenario-based approach. Appl Soft Comput 2019;75:616–32.
[36] Abaza A, Fawzy A, El-Sehiemy RA, Alghamdi AS, Kamel S. Sensitive reactive power dispatch solution accomplished with renewable energy allocation using

an enhanced coyote optimization algorithm. Ain Shams Eng J 2021;12 (2):1723–39.
[37] Abdel-Fatah S, Ebeed M, Kamel S, October YJ. Reactive power dispatch solution with optimal installation of renewable energy resources considering uncertainties. In: In 2019 IEEE Conference on Power Electronics and Renewable Energy (CPERE). IEEE; 2019. p. 118–23. doi: https://doi.org/10.1109/CPERE45374.2019.8980056.
[38] Ebeed M, Ali A, Mosaad MI, Kamel S. An improved lightning attachment procedure optimizer for optimal reactive power dispatch with uncertainty in renewable energy resources. IEEE Access 2020;8:168721–31.
[39] Faramarzi A, Heidarinejad M, Mirjalili S, Gandomi AH. Marine Predators Algorithm: A nature-inspired metaheuristic. Expert Systems with Applications. Expert Syst Appl 2020;152:113377. doi: https://doi.org/10.1016/j.eswa.2020.113377.
[40] Abdel-Basset M, El-Shahat D, Chakrabortty RK, Ryan M. Parameter estimation of photovoltaic models using an improved marine predators algorithm. Energy Convers Manage 2021;227:113491. doi: https://doi.org/10.1016/j.enconman.2020.113491.
[41] Abd Elaziz M, Ewees AA, Yousri D, Alwerfali HSN, Awad QA, Lu S, et al. An improved Marine Predators algorithm with fuzzy entropy for multi-level thresholding: Real world example of COVID-19 CT image segmentation. IEEE Access 2020;8:125306–30.
[42] Soliman MA, Hasanien HM, Alkuhayli A. Marine Predators Algorithm for Parameters Identification of Triple-Diode Photovoltaic Models. IEEE Access 2020;8:155832–42.
[43] Abdel-Basset M, Mohamed R, Elhoseny M, Chakrabortty RK, Ryan M. A hybrid COVID-19 detection model using an improved marine predators algorithm and a ranking-based diversity reduction strategy. IEEE Access 2020;8:79521–40.
[44] Al-Qaness MA, Ewees AA, Fan H, Abualigah L, Abd Elaziz M. Marine predators algorithm for forecasting confirmed cases of COVID-19 in Italy, USA, Iran and Korea. Int J Environ Res Public Health 2020;17(10):3520.
[45] Diab AAZ, Tolba MA, El-Magd AGA, Zaky MM, El-Rifaie AM. Fuel Cell Parameters Estimation via Marine Predators and Political Optimizers. IEEE Access 2020;8:166998–7018.
[46] Ebeed M, Alhejji A, Kamel S, Jurado F. Solving the Optimal Reactive Power Dispatch Using Marine Predators Algorithm Considering the Uncertainties in Load and Wind-Solar Generation Systems. Energies 2020;13(17):4316.
[47] Humphries NE, Queiroz N, Dyer JR, Pade NG, Musyl MK, Schaefer KM, et al. Environmental context explains Lévy and Brownian movement patterns of marine predators. Nature 2010;465(7301):1066–9.
[48] Nasouri Gilvaei M, Jafari H, Jabbari Ghadi M, Li Li. A novel hybrid optimization approach for reactive power dispatch problem considering voltage stability index. Eng Appl Artif Intell 2020;96:103963. doi: https://doi.org/10.1016/j.engappai.2020.103963.
[49] Mandal, S.; Mandal, K.K.; Kumar, S. A new optimization technique for optimal reactive power scheduling using Jaya algorithm. In 2017 Innovations in Power and Advanced Computing Technologies (i-PACT). *IEEE* **2017**, 1-5.
[50] Ela AAAE, Abido MA, Spea SR. Differential evolution algorithm for optimal reactive power dispatch. Electr Power Syst Res 2011;81(2):458–64.
[51] Suresh V, Kumar SS. Optimal reactive power dispatch for minimization of real power loss using SBDE and DE-strategy algorithm. J Ambient Intell Hum Comput 2020:1–15. doi: https://doi.org/10.1007/s12652-020-02673-w.
[52] Shaheen MAM, Hasanien HM, Alkuhayli A. A novel hybrid GWO-PSO optimization technique for optimal reactive power dispatch problem solution. Ain Shams Eng J 2021;12(1):621–30.
[53] Ben oualid Medani K, Sayah S, Bekrar A. Whale optimization algorithm based optimal reactive power dispatch: A case study of the Algerian power system. Electr Power Syst 2018;163:696–705.
[54] Khazali AH, Kalantar M. Optimal reactive power dispatch based on harmony search algorithm. Int J Electr Power Energy Syst 2011;33(3):684–92.
[55] Shaheen MA, Yousri D, Fathy A, Hasanien HM, Alkuhayli A, Muyeen SM. A Novel Application of Improved Marine Predators Algorithm and Particle Swarm Optimization for Solving the ORPD Problem. Energies 2020;13 (21):5679.
[56] Sahli Z, Hamouda A, Bekrar A, Trentesaux D. Reactive power dispatch optimization with voltage profile improvement using an efficient hybrid algorithm. Energies 2018;11(8):2134.
[57] Rajan A, Malakar T. Optimal reactive power dispatch using hybrid Nelder-Mead simplex-based firefly algorithm. Int J Electr Power Energy Syst 2015;66:9–24.
[58] Polprasert J, Ongsakul W, Dieu VN. Optimal reactive power dispatch using improved pseudo-gradient search particle swarm optimization. Electr Power Compon Syst 2016;44(5):518–32.
[59] Li Z, Cao Y, Dai LV, Yang X, Nguyen TT. Finding solutions for optimal reactive power dispatch problem by a novel improved antlion optimization algorithm. Energies 2019;12(15):2968.
[60] Nguyen TT, Vo DN. Improved social spider optimization algorithm for optimal reactive power dispatch problem with different objectives. Neural Comput Appl. 2020;32:5919–50.
[61] Lenin K. Hybridization of Genetic Particle Swarm Optimization Algorithm with Symbiotic Organisms Search Algorithm for Solving Optimal Reactive Power Dispatch Problem. J Appl Sci Eng Technol Education 2021;3(1):12–21.
[62] Chen G, Liu L, Zhang Z, Huang S. Optimal reactive power dispatch by improved GSA-based algorithm with the novel strategies to handle constraints. Appl Soft Comput 2017;50:58–70.
[63] Aljohani TM, Ebrahim AF, Mohammed O. Single and multiobjective optimal reactive power dispatch based on hybrid artificial physics–particle swarm optimization. Energies 2019;12(12):2333.
[64] Khan NH, Wang Y, Tian De, Jamal R, Iqbal S, Saif MAA, et al. A Novel Modified Lightning Attachment Procedure Optimization Technique for Optimal Allocation of the FACTS Devices in Power Systems. IEEE Access 2021;9:47976–97.
[65] Khan NH, Wang Y, Tian De, Jamal R, Kamel S, Ebeed M. Optimal Siting and Sizing of SSSC Using Modified Salp Swarm Algorithm Considering Optimal Reactive Power Dispatch Problem. IEEE Access 2021;9:49249–66.
[66] Elavarasan RM, Shafiullah GM, Padmanaban S, Kumar NM, Annam A, Vetrichelvan AM, et al. A comprehensive review on renewable energy development, challenges, and policies of leading Indian states with an international perspective. IEEE Access 2020;8:74432–57.
[67] Madurai Elavarasan R, Afridhis S, Vijayaraghavan RR, Subramaniam U, Nurunnabi M. SWOT analysis: A framework for comprehensive evaluation of drivers and barriers for renewable energy development in significant countries. Energy Rep 2020;6:1838–64.